2019 IEEE 16th International Conference on Rehabilitation Robotics (ICORR)
Toronto, Canada, June 24-28, 2019

A Support Vector Regression Approach for Continuous Prediction of Ankle Angle and Moment During Walking: An Implication for Developing a Control Strategy for Active Ankle Prostheses

Sharmita Dey[1], Mahdy Eslamy[1], Takashi Yoshida[1], Michael Ernst[2], Thomas Schmalz[2], Arndt F. Schilling[1]

Abstract— **Lower limb amputations impair normal locomotion. This calls for the use of prosthetic devices to restore the lost or disabled functionality. Most of the commercially available prostheses offer only passive assistance with limited capacity. On the other hand, active prostheses may better restore movement, by supporting missing muscle function with additional motor power. The control algorithms of such embedded motors must understand the users locomotive intention to produce the required locomotion similar to that of an able-bodied individual. For individuals with transtibial amputation, the control algorithm should produce the desired locomotion by controlling an active ankle joint to generate appropriate ankle angle and ankle moment.**

In this paper, a strategy is proposed for the continuous estimation of ankle angle and ankle moment during walking using a support vector regression approach. Experimentally obtained hip and knee joint motion data were provided as the inputs to the support vector regression model. It is shown that, for level ground walking at self-selected speed, the proposed method could predict the ankle angle and moment with high accuracy (mean R^2 value of 0.98 for ankle angle and 0.97 for ankle moment).

I. INTRODUCTION

Lower limb amputations impair normal locomotion. In Germany alone, there are more than fifty thousand lower limb amputations per year according to a recent study [1]. In order to restore the lost or disabled locomotive functionality, amputees use prosthetic devices. Most of the commercially available prosthetic devices offer only passive assistance [2]. Even though passive prosthetic feet can store and release energy during push off [3], they do not produce power with an adequate pattern for normal gait [4]. Any abnormalities in the prosthetic output have to be compensated by the intact/residual body parts which leads to increased gait metabolism and asymmetric gait patterns [2]. On the other hand, an active or powered prosthesis can produce mechanical power using motors and thus have the potential to produce more human like locomotion [2]. The control algorithms of an active prosthetic device should be able to interpret the user's locomotive intention and control the actuator to produce the desired locomotion.

[1] Applied Rehabilitation Technology Lab (ART-Lab), Department of Trauma Surgery, Orthopedics and Plastic Surgery, University Medical Center Goettingen, Goettingen, Germany

[2] Research Biomechanics, Clinical Research & Services, Ottobock SE & Co. KGaA, Goettingen, Germany

Any correspondences should be sent to sharmita.dey [at] med.uni-goettingen.de

Development of such control algorithms is a challenging task. These are typically implemented by using a multilevel control approach, in which the control is achieved on three levels: high, mid, and low [5], [6], [7]. The high-level controller uses inputs from sensors worn on residual limb parts [8] or the prosthetic device [9] to deduce the locomotive intentions of the user (e.g., walking or climbing). At the mid level, finite state controllers are commonly used to determine the necessary kinematics or dynamics (i.e., a state) for the intended locomotion mode recognized at the high level [5], [7]. In this case, the gait cycle is divided into discrete phases, and each phase is associated with a specific state. Thus, an appropriate transition between these phases must also be defined by switching rules. At the lowest level, the device is actuated to achieve the required joint motion or actuator trajectory for the assigned state [6]. Because the finite state controller must choose from a finite number of predefined discrete states, the above-mentioned multilevel approach is inherently limited [10].

A relatively new approach is the continuous control which eliminates the need for a mid-level state-based control. Input data like EMG signals [10], thigh motion data [11], and shank motion data [12], [13] are used to continuously estimate the outputs like the prosthetic ankle mechanics [10], knee and ankle kinematics [11], or motor positions [13]. In [14], hip, knee and ankle kinematics were modeled as a continuous function of gait phase, gait speed and incline. In [15], Gaussian process regression was used to estimate the power required at ankle joint as a function of the speed and position in the gait cycle. All of these methods do not require division of gait cycle into discrete phases.

In this study, we aim to develop a strategy for continuously predicting the ankle angle and moment during level-ground walking by using a support vector regression (SVR) model. The SVR model is trained to learn the non-linear input-output relationship and use hip and knee joint kinematics to continuously predict the ankle angle and ankle moment on unseen level walking datasets. Thus, our model eliminates the need for determining gait phases and using switching rules.

We have chosen SVR for the control algorithm because it has proven to be effective in real-valued function estimation, offers excellent generalization ability to unseen datasets with high prediction accuracy, and is computationally efficient for increasing input dimensions because the computational complexity of SVR is independent of the dimensionality

978-1-7281-2755-2/19/$31.00 ©2019 IEEE

of the input space [16], [17]. Further, to the best of our knowledge, SVR has not been previously used for predicting ankle angles and moments in the context of continuous control. Also, we have chosen to use hip and knee motion data as inputs to the SVR model. Since locomotion requires multi-joint coordination [18], we assume that the motion data from the intact lower extremity joints can be used to infer an individual's gait. Thus, our study combines two objectives. First, to develop a control strategy using SVR as a model to continuously predict the ankle angles and moments during level ground walking. Second, to examine the feasibility of using motion of the intact lower limb joints (hip and knee) as input instead of the residual limb where the prosthesis is worn (e.g., shank).

This approach has potential implications for devising a controller for an active prosthetic ankle for assisting locomotion in transtibial amputees whose intact joints (hip and knee) on the prosthetic side can be used to estimate the kinematics and dynamics of an active prosthetic ankle.

II. METHODOLOGY

The study was approved by the local ethics committee, University Medical Center Goettingen (application number: 18/03/26). In the first step, biomechanical data were recorded during walking trials and analyzed to calculate the lower limb joint kinematics and dynamics. In the second step, an SVR model was trained to predict the ankle angle and ankle moment from the given inputs (hip and knee joint motion data).

A. Biomechanical data acquisition and analysis

Biomechanical data were acquired from a healthy subject (male, body mass: 56.5kg) while he performed level walking trials at self-selected walking speeds in a gait laboratory. Three-dimensional motion data were recorded using a motion capture system (Vicon Motion Systems, Ltd., UK) with retro-reflective markers and twelve infrared cameras. Data acquisition software Nexus (Vicon Motion Systems, Ltd., UK) was used for data recording. The motion data were captured at 200 Hz. Sixteen walking trials (4-second epochs) were recorded. The marker data were also recorded in a static pose. Along with the three-dimensional motion capture data, the ground reaction forces (GRF) were measured using two force plates (9287A, Kistler Group, Switzerland) at 1 kHz. For each trial, data from one gait cycle (between two consecutive right heel contacts), during which GRF measurements were recorded, were considered for further analysis.

Biomechanical data analysis was performed to calculate the joint kinematics and dynamics from the motion capture data and GRF. The open-source biomechanical modeling, simulation and analysis software (OpenSim) [19] was used for the analysis. The scaling tool in OpenSim was used to scale the generic model for the subject. Further, the scaled model and the experimental marker trajectories were fed into the inverse kinematics tool of OpenSim which yielded the joint angles relevant for our study. The calculated kinematics data and GRF was fed into the inverse dynamics tool to calculate the corresponding joint moments. The joint angles and moments that were calculated during this study were comparable to the results available in literature [20], [21].

B. Support Vector Regression

In a regression problem, the goal is to learn an underlying mathematical relationship between the given input observations (in our case, hip and knee joint motion data) and the corresponding target/output values (ankle angles and moments). The support vector regression (SVR) is a generalization of the support vector machine approach [22] for solving regression problems. The SVR problem can be summarized as finding a function, $f(x)$, such that $|y_i - f(x_i)| \leq \varepsilon$. The basic idea of SVR is presented below.

Let $X = \{(x_i, y_i), i = 1,..,N\} \subset \chi \times \mathbb{R}$ represent the training data, where $x_i \in \chi, i = 1,..,N$ represents the inputs and $y_i, i = 1,..,N$ represents the corresponding outputs or targets. Here, $\chi = \mathbb{R}^d$ represents the input space. In ε- SVR [23], the goal is to find a function (affine case),

$$f(x) = \langle w, x \rangle + b \text{ with } w \in \chi, b \in \mathbb{R} \tag{1}$$

(where w represents weight and b is the threshold), such that for all training inputs $x_i, i = 1..N$, the deviation of $f(x)$ from the actual target y_i is less than ε while $f(x)$ being as smooth as possible. This can be formulated as a convex optimization problem:

$$\begin{aligned} \text{minimize } & \frac{1}{2}||w||^2 + C\sum_{i=1}^{N}(\zeta_i + \zeta_i^*) \\ \text{subject to } & y_i - \langle w, x_i \rangle - b \leq \varepsilon + \zeta_i, \\ \text{and } & \langle w, x_i \rangle + b - y_i \leq \varepsilon + \zeta_i^*, \\ \text{and } & \zeta_i, \zeta_i^* \geq 0, \end{aligned} \tag{2}$$

where ζ and ζ^* are slack variables introduced to relax the constraints and make the optimization feasible. C is a trade-off between the smoothness of function, f, and the amount up to which errors larger than ε are allowed. The Lagrangian L can be formed as follows:

$$\begin{aligned} L := \frac{1}{2}\|w\|^2 + C\sum_{i=1}^{N}(\zeta_i + \zeta_i^*) - \sum_{i=1}^{N}(\eta_i\zeta_i + \eta_i^*\zeta_i^*) \\ - \sum_{i=1}^{N}\alpha_i(\varepsilon + \zeta_i - y_i + \langle w, x_i \rangle + b) \\ - \sum_{i=1}^{N}\alpha_i^*(\varepsilon + \zeta_i^* + y_i - \langle w, x_i \rangle - b) \end{aligned} \tag{3}$$

where $\eta_i, \eta_i^*, \alpha_i$, and $\alpha_i^* \geq 0$ are Lagrange multipliers. At the saddle point, the partial derivatives of the Lagrangian with respect to the primal variables, w, b, ζ_i, and ζ_i^* becomes zero. Substituting the results in Eq. 3 gives the dual formulation

$$\begin{aligned}\text{minimize } & \frac{1}{2}\sum_{i,j=1}^{N}(\alpha_i-\alpha_i^*)(\alpha_j-\alpha_j^*)\langle x_i,x_j\rangle \\ & +\varepsilon\sum_{i=1}^{N}(\alpha_i+\alpha_i^*)-\sum_{i=1}^{N}y_i(\alpha_i-\alpha_i^*) \\ \text{subject to } & \sum_{i=1}^{N}(\alpha_i-\alpha_i^*)=0, \text{ and } \alpha_i,\alpha_i^*\in[0,C].\end{aligned} \tag{4}$$

At the optimal solution,

$$\begin{aligned}w &= \sum_{i=1}^{N}(\alpha_i-\alpha_i^*)x_i, \text{ and thus,} \\ f(x) &= \sum_{i=1}^{N}(\alpha_i-\alpha_i^*)\langle x_i,x\rangle+b\end{aligned} \tag{5}$$

Thus, w can be expressed as a linear combination of a subset of input patterns, x_i. This is called the *Support Vector expansion* [17]. The complexity of the decision function, $f(x)$, does not depend on the dimensionality of the input, but only on the number of support vectors [17]. The term, b, is computed using the Karush-Kuhn-Tucker (KKT) conditions, which states that at the point of the solution, the product of dual variables and constraints vanish. These conditions can be summarized as

$$\begin{aligned}\alpha_i(\varepsilon+\zeta_i-y_i+\langle w,x_i\rangle+b)&=0 \\ \alpha_i^*(\varepsilon+\zeta_i^*+y_i-\langle w,x_i\rangle-b)&=0\end{aligned} \tag{6}$$

and

$$\begin{aligned}(C-\alpha_i)\zeta_i&=0 \\ (C-\alpha_i^*)\zeta_i^*&=0\end{aligned} \tag{7}$$

For a more detailed explanation on the computation of b, see [17].

In order to perform a non-linear regression, the input patterns, x_i, are mapped into a feature space, F, by a mapping, $\Phi:\chi\rightarrow F$, and applying the standard SVR in the feature space.

In the nonlinear case, the dual problem becomes

$$\begin{aligned}\text{minimize } & \frac{1}{2}\sum_{i,j=1}^{N}(\alpha_i-\alpha_i^*)(\alpha_j-\alpha_j^*)k(x_i,x_j) \\ & +\varepsilon\sum_{i=1}^{N}(\alpha_i+\alpha_i^*)-\sum_{i=1}^{N}y_i(\alpha_i-\alpha_i^*) \\ \text{subject to } & \sum_{i=1}^{N}(\alpha_i-\alpha_i^*)=0, \text{ and } \alpha_i,\alpha_i^*\in[0,C]\end{aligned} \tag{8}$$

where $k(x,x')=\langle\Phi(x),\Phi(x')\rangle$ is the kernel function. The decision function can be formulated as

$$f(x)=\sum_{i=1}^{N}(\alpha_i-\alpha_i^*)k(x_i,x)+b \tag{9}$$

C. Inputs and Outputs for the SVR model

Time series measurements of hip and knee angles (θ_{hip}, θ_{knee}) and angular velocities ($\dot{\theta}_{hip}$, $\dot{\theta}_{knee}$) during one gait cycle were used as inputs to the SVR model. The corresponding ankle angles and ankle moments were the targets or outputs for the SVR model. The hip and knee joint angles were obtained by performing inverse kinematics on the motion capture data. The joint angular velocities were obtained by finite difference method. Different combination of these features were provided as inputs to the SVR model. These combinations stated below, formed different input test cases

- Case I: 2 inputs (θ_{hip}, θ_{knee})
- Case II: 3 inputs (θ_{hip}, θ_{knee}, $\dot{\theta}_{knee}$)
- Case III: 4 inputs (θ_{hip}, θ_{knee}, $\dot{\theta}_{knee}$, $\dot{\theta}_{hip}$)

Our algorithm was required to continuously predict the values of ankle angle, θ_{ankle}, and ankle moment, τ_{ankle}, as outputs for each of the above cases. The predicted values were compared against those calculated from measurements (target values). Fig. 1 shows the model inputs: hip and knee angles as well as the angular velocities during one gait cycle.

D. Training and validation of the SVR model

The input features were low-pass filtered using a Butterworth filter with a 6-Hz cut-off frequency to remove the noise. The training inputs were then normalized within the range, [0,1], by min-max scaling. In order to suit a real-time scenario, the unseen test inputs were also normalized to the maximum of the training inputs. An SVR model was trained using the inputs and targets described in section II-C to learn the relationship between them. A Gaussian (*rbf*) kernel [24] was used in our work and the parameter, C, of the SVR model was chosen using grid search cross validation [25]. A k-fold (k=16) cross validation method was used for assessing the performance of the model, where in each step, the model was trained using datasets from (k-1) trials and tested on the dataset from the remaining trial. The performance of the SVR model was evaluated by comparing the predicted values of ankle angle and ankle moment to those calculated from inverse kinematics and inverse dynamics, respectively.

Two commonly used performance metrics, the coefficient of determination, R^2 and root mean square error (*RMSE*) were used to evaluate the performance of the SVR model. We also present a gait phase specific error analysis to have a better understanding of *RMSE* distribution across different sections of the gait cycle. Therefore, *RMSE* was examined within seven different phases of the gait cycle: loading response (0-10%), mid stance (10-30%), terminal stance (30-50%), pre-swing (50-60%), initial swing (60-75%), mid swing (75-87%), and terminal swing (87-100%). In each phase, the mean *RMSE* across all trials was calculated. It is to be noted that our prediction was continuous and did not require the division of the gait cycle into phases. The gait phase specific error analysis is done only to give an estimation of the performance of our model in different phases of the gait cycle.

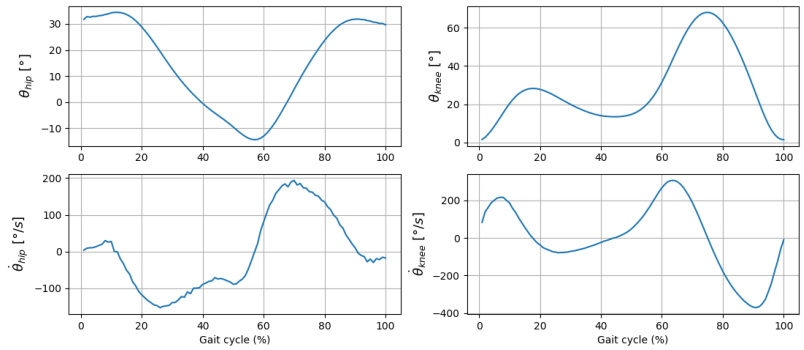

Fig. 1. Input data for one gait cycle of a walking trial. Hip angle and knee angle (top) were calculated from the biomechanical marker data using inverse kinematics tool of OpenSim. These were differentiated (bottom) to obtain further input features to the SVR model.

III. RESULTS

Table I shows the R^2 values and *RMSE* of the SVR model in predicting the ankle angle and ankle moment for different input cases. Both the R^2 values and *RMSE* are averaged across all the trials. The results show that the proposed algorithm predicted the ankle angle and ankle moment with high levels of accuracy in all three input test cases.

By providing only two inputs to the SVR model ($\theta_{hip}, \theta_{knee}$), a mean R^2 value of 0.95 was obtained in both ankle angle and moment prediction. Values above 0.91 were obtained for all the 16 trials. Mean *RMSE* of 2.17° was obtained for angle prediction (min. *RMSE* = 1.52°, max. *RMSE* = 3.02°). For ankle moment prediction, a mean *RMSE* of 0.11 Nm/kg was obtained (min. *RMSE* = 0.05 Nm/kg, max. *RMSE* = 0.16 Nm/kg). It can also be seen that the predicted patterns of ankle angle and ankle moment follows the target/measured values closely (Fig. 2 Case I) except for deviations in middle and end of the gait cycle for the ankle angle and towards the first half of the gait cycle for the ankle moment. A gait phase specific analysis showed that more errors occur in pre-swing and terminal swing phase for ankle angle prediction and mid stance and terminal stance phases for ankle moment prediction (Fig 3 Case I).

When the knee angular velocity ($\dot{\theta}_{knee}$) was provided as an additional input to the SVR model, improvement in ankle angle prediction was observed compared to Case I. This improvement was marked by higher R^2 values and lower *RMSE* than Case I. Mean R^2 value of 0.97 was obtained with an R^2 above 0.93 for all trials. The *RMSE* across all the trials averaged to 1.67°, which was much lower compared to Case I. The lowest and highest *RMSE*s also reduced compared to Case I. The ankle moment prediction also showed an improvement compared to Case I, with a mean *RMSE* of 0.10 Nm/kg and mean R^2 value of 0.96. The predicted values more closely followed the measured values compared to case I (see Fig. 2 Case II). The deviations in the predicted values towards the end of gait cycle has reduced for both ankle angle and ankle moment. This can also be observed from the reduction in error during the terminal swing phase (Fig 3 Case II) for both ankle angle and ankle moment estimations. In addition, the *RMSE* in ankle angle during pre-swing phase and ankle moment during mid stance phase reduced compared to Case I.

By providing all four input features, ($\theta_{hip}, \theta_{knee}$, $\dot{\theta}_{knee}$, and $\dot{\theta}_{hip}$) to the SVR model, further improvement was observed in both the ankle angle and the ankle moment prediction. Mean R^2 value for ankle angle prediction increased to 0.98 while minimum R^2 value increased to 0.97. For ankle moment prediction, mean and minimum R^2 values increased to 0.97 and 0.95 respectively. Mean *RMSE* decreased to 1.29°(θ_{ankle}) and 0.08 Nm/kg (τ_{ankle}). The maximum *RMSE* for ankle angle and ankle moment also reduced compared to Cases I or II. The predicted values of ankle angle and ankle moment most accurately aligned with the measured values in this case (Fig 2 Case III). The *RMSE* in ankle angle estimation stayed below 2° during all gait phases, with a visible decrease in *RMSE* during pre-swing phase (Fig. 3 Case III θ_{ankle}). In ankle moment prediction, noticeable errors still occured in the mid- and terminal- stance phase (Fig. 3 Case III τ_{ankle}). However, the *RMSE* values were reduced compared to Cases I and II.

IV. DISCUSSION

The results of our study suggest that it is possible to continuously predict the ankle kinematics and dynamics during level walking from hip and knee motion data by using an SVR model. It was seen that even when using only two inputs (hip and knee angle), high accuracy of prediction was obtained for both ankle angle and ankle moment (mean $R^2 = 0.95$). Using two additional inputs (hip and knee angular velocities), prediction accuracies of ankle angle and ankle moment could be improved further. Although the hip and knee angles alone could achieve an $R^2 > 0.9$ (best possible score being 1), additional inputs were necessary to improve the alignment of temporal patterns to the target values, particularly in the case of ankle moments. The proposed algorithm could be used to devise a control strategy for an active prosthetic ankle for transtibial amputees whose intact joints (hip and knee) on the prosthetic side can

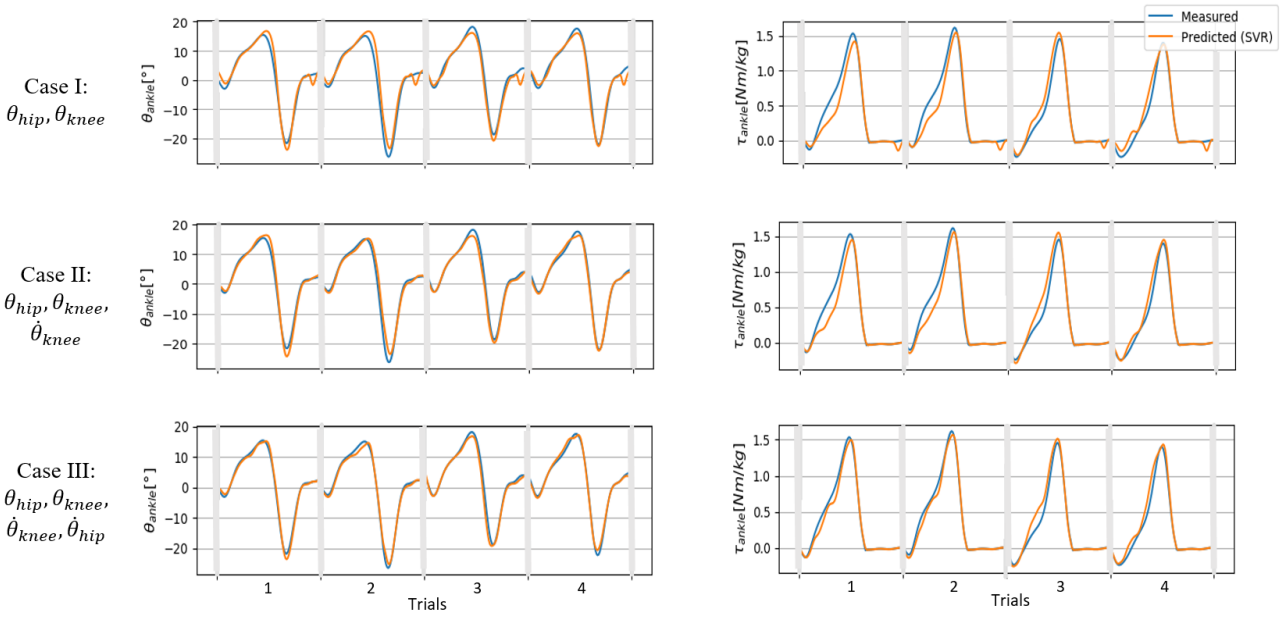

Fig. 2. Ankle angle, θ_{ankle}, and ankle moment, τ_{ankle}, for four separate gait cycles of normal walking with different inputs (cases) to SVR model. The blue curves represent the measured/target values of θ_{ankle}, τ_{ankle} calculated by inverse kinematics and dynamics respectively. The orange curves show the prediction of these values by the trained SVR model. The inputs to the model in each case are indicated on the left.

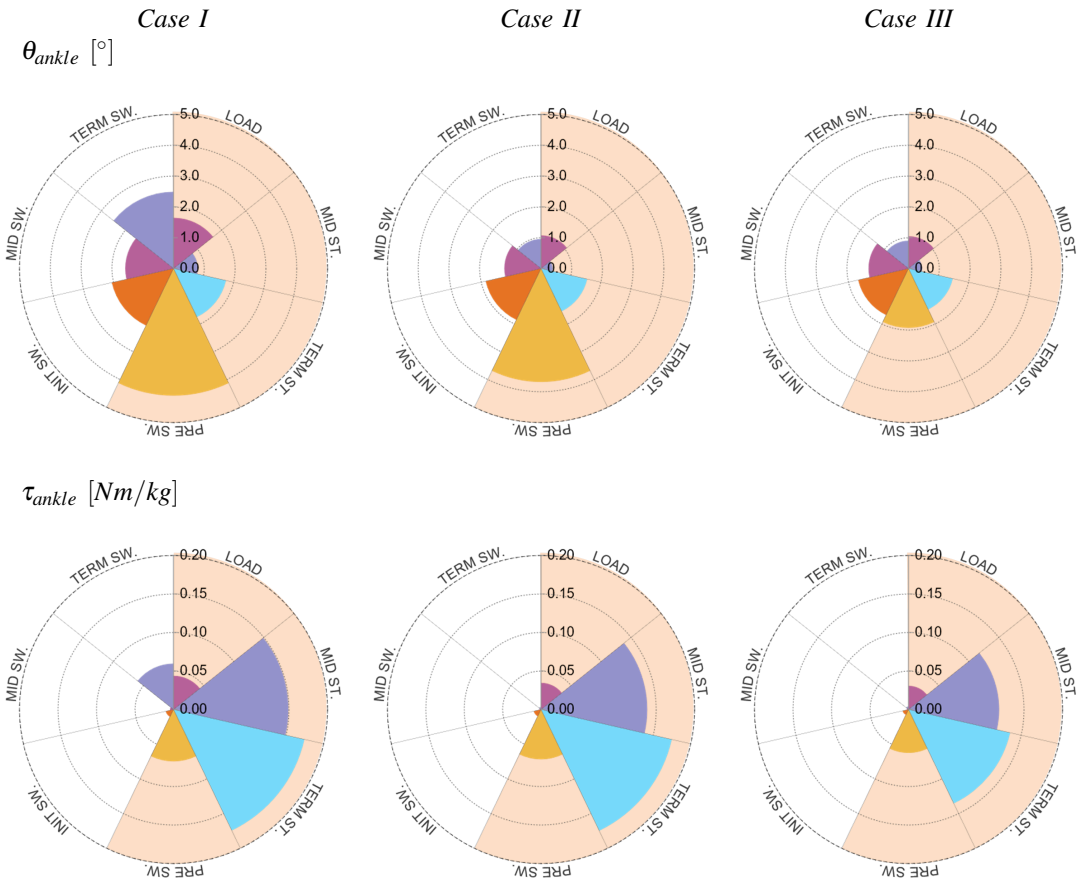

Fig. 3. The radial bar charts showing a gait phase specific error analysis *RMSE* of the continuous prediction of ankle angle (top) and ankle moment (bottom) for different input test cases. Each gait cycle is represented as seven different phases depending on the gait percentage: loading response (0-10%), mid stance (10-30%), terminal stance (30-50%), pre-swing (50-60%), initial swing (60-75%), mid swing (75-87%) and terminal swing (87-100%). The entire stance and pre-swing phase is indicated by the shaded region.

TABLE I

R^2 VALUES AND *RMSE* OF SVR MODEL PREDICTIONS WITH DIFFERENT INPUTS

Case	Inputs	Output	$\overline{R^2}$	R^2_{min}	R^2_{max}	$\overline{RMSE}$	$RMSE_{min}$	$RMSE_{max}$
I	θ_{hip}, θ_{knee}	θ_{ankle}	0.95	0.91	0.98	2.17°	1.52°	3.02°
		τ_{ankle}	0.95	0.91	0.99	0.11 Nm/kg	0.05 Nm/kg	0.16 Nm/kg
II	θ_{hip}, θ_{knee}, $\dot{\theta}_{knee}$	θ_{ankle}	0.97	0.93	0.99	1.67°	0.78°	2.48°
		τ_{ankle}	0.96	0.93	0.98	0.10 Nm/kg	0.06 Nm/kg	0.14 Nm/kg
III	θ_{hip}, θ_{knee}, $\dot{\theta}_{knee}$, $\dot{\theta}_{hip}$	θ_{ankle}	0.98	0.97	0.99	1.29°	0.80°	1.93°
		τ_{ankle}	0.97	0.95	0.99	0.08 Nm/kg	0.05 Nm/kg	0.12 Nm/kg

provide inputs to generate continuous control commands. To utilize our approach, the input data to the algorithm has to be obtained from joints that are extrinsic to the prosthesis. Even though using intrinsic sensors makes it easier to don and doff the prosthesis, the advancements in wearable sensor technology have made it possible to obtain joint angle measurements by using light weight sensors directly embroidered into a fabric. Since these sensors can be integrated into the users clothes, they can be worn with ease and comfort. Thus, using extrinsic sensors could provide useful information for prosthetic control from the intact body parts without compromising the user's comfort. Different wearable sensors using knitted piezoelectric fabrics (KPF) [26], conductive fibres [27], and strain sensors [28] have been proposed for measuring joint angles. Wearable goniometers and stretch sensors [29], [30], [31] as well as miniaturised IMU sensors [32] for measuring joint angles are also available commercially. Another noteworthy point is that calculating velocities using the finite difference method in real-time can lead to a lag in velocity data. To minimize this effect, a higher sampling frequency could be used for velocity calculation in real-time. Alternatively, a combination of wearable goniometer and gyroscope could also be used to measure the angle and angular velocity respectively.

There were a few limitations to our study. First, the algorithm is validated only on level-walking datasets from one healthy subject. Further research should validate this approach on a larger pool of healthy and amputee data for both subject specific and inter-subject predictions. Second, the biomechanical data was obtained in a laboratory using retroreflective markers. While this method can provide reliable measurements of joint kinematics, this data acquisition method is not feasible in real-life locomotive conditions. In a real-life scenario, wearable sensors have to be used for data acquisition. The wearable sensors may be affected by specific artifacts, which were not taken into consideration in this study. Third, the proposed model is trained for predicting the ankle kinematics and dynamics during level-ground walking. Performance of our approach for other locomotion modes like on uneven grounds or stairs needs to be evaluated.

V. CONCLUSION AND FUTURE SCOPE

We have designed a strategy for the continuous prediction of ankle angle and ankle moment using an SVR model. Hip and knee joint motion data were provided as inputs to the model. The model performance evaluated on datasets recorded during level walking trials gave promising results suggesting that our approach can be used to design control strategies for active ankle prosthesis. Future research would focus on validating the approach on a larger sample of healthy and amputee subjects over different locomotion modes and speeds. Additionally, the algorithm has to be validated in real time with data acquired using wearable sensors instead of motion capture data as done in this study. The robustness of the algorithm to the changes in prosthetic setup should also be evaluated. If these steps are successful, the algorithm could be implemented for controlling an active ankle in real time.

ACKNOWLEDGMENT

This work was partially supported by the grant (INOPRO-16SV7656) from the German Federal Ministry of Education and Research to A. F. Schilling.

REFERENCES

[1] K. Kröger, C. Berg, F. Santosa, N. Malyar, and H. Reinecke, "Lower limb amputation in germany: An analysis of data from the german federal statistical office between 2005 and 2014," *Deutsches Ärzteblatt International*, vol. 114, no. 8, p. 130, 2017.

[2] S. Au, M. Berniker, and H. Herr, "Powered ankle-foot prosthesis to assist level-ground and stair-descent gaits," *Neural Networks*, vol. 21, no. 4, pp. 654–666, 2008.

[3] A. Gitter, J. M. Czerniecki, and D. M. DeGroot, "Biomechanical analysis of the influence of prosthetic feet on below-knee amputee walking.," *American journal of physical medicine & rehabilitation*, vol. 70, no. 3, pp. 142–148, 1991.

[4] M. Windrich, M. Grimmer, O. Christ, S. Rinderknecht, and P. Beckerle, "Active lower limb prosthetics: a systematic review of design issues and solutions," *Biomedical engineering online*, vol. 15, no. 3, p. 140, 2016.

[5] M. R. Tucker, J. Olivier, A. Pagel, H. Bleuler, M. Bouri, O. Lambercy, J. d. R. Millán, R. Riener, H. Vallery, and R. Gassert, "Control strategies for active lower extremity prosthetics and orthotics: a review," *Journal of NeuroEngineering and Rehabilitation*, vol. 12, p. 1, Jan 2015.

[6] H. A. Varol, F. Sup, and M. Goldfarb, "Multiclass real-time intent recognition of a powered lower limb prosthesis," *IEEE Transactions on Biomedical Engineering*, vol. 57, no. 3, pp. 542–551, 2010.

[7] F. Sup, A. Bohara, and M. Goldfarb, "Design and control of a powered transfemoral prosthesis," *The International journal of robotics research*, vol. 27, no. 2, pp. 263–273, 2008.

[8] H. Huang, T. A. Kuiken, R. D. Lipschutz, *et al.*, "A strategy for identifying locomotion modes using surface electromyography," *IEEE Transactions on Biomedical Engineering*, vol. 56, no. 1, pp. 65–73, 2009.

[9] H. A. Varol, F. Sup, and M. Goldfarb, "Real-time gait mode intent recognition of a powered knee and ankle prosthesis for standing and walking," in *2008 2nd IEEE RAS & EMBS International Conference on Biomedical Robotics and Biomechatronics*, pp. 66–72, IEEE, 2008.
[10] S. Huang, *Continuous Proportional Myoelectric Control of an Experimental Powered Lower Limb Prosthesis During Walking Using Residual Muscles.* PhD thesis, 2014.
[11] D. Quintero, D. J. Villarreal, and R. D. Gregg, "Preliminary experiments with a unified controller for a powered knee-ankle prosthetic leg across walking speeds," in *2016 IEEE/RSJ International Conference on Intelligent Robots and Systems (IROS)*, pp. 5427–5433, IEEE, 2016.
[12] M. A. Holgate, T. G. Sugar, and A. W. Bohler, "A novel control algorithm for wearable robotics using phase plane invariants," in *Robotics and Automation, 2009. ICRA'09. IEEE International Conference on*, pp. 3845–3850, IEEE, 2009.
[13] M. Eslamy and A. F. Schilling, "A conceptual high level controller to walk with active foot prostheses/orthoses," in *2018 7th IEEE International Conference on Biomedical Robotics and Biomechatronics (Biorob)*, pp. 1224–1229, IEEE, 2018.
[14] K. R. Embry, D. J. Villarreal, R. L. Macaluso, and R. D. Gregg, "Modeling the kinematics of human locomotion over continuously varying speeds and inclines," *IEEE transactions on neural systems and rehabilitation engineering*, vol. 26, no. 12, pp. 2342–2350, 2018.
[15] N. Dhir, H. Dallali, E. M. Ficanha, G. A. Ribeiro, and M. Rastgaar, "Locomotion envelopes for adaptive control of powered ankle prostheses," in *2018 IEEE International Conference on Robotics and Automation (ICRA)*, pp. 1488–1495, IEEE, 2018.
[16] M. Awad and R. Khanna, *Support Vector Regression*, pp. 67–80. Berkeley, CA: Apress, 2015.
[17] A. J. Smola and B. Schölkopf, "A tutorial on support vector regression," *Statistics and computing*, vol. 14, no. 3, pp. 199–222, 2004.
[18] A. M. Boudali, P. J. Sinclair, R. Smith, and I. R. Manchester, "Human locomotion analysis: Identifying a dynamic mapping between upper and lower limb joints using the koopman operator," in *2017 39th Annual International Conference of the IEEE Engineering in Medicine and Biology Society (EMBC)*, pp. 1889–1892, IEEE, 2017.
[19] S. L. Delp, F. C. Anderson, A. S. Arnold, P. Loan, A. Habib, C. T. John, E. Guendelman, and D. G. Thelen, "Opensim: open-source software to create and analyze dynamic simulations of movement," *IEEE transactions on biomedical engineering*, vol. 54, no. 11, pp. 1940–1950, 2007.
[20] R. Riener, M. Rabuffetti, and C. Frigo, "Stair ascent and descent at different inclinations," *Gait & posture*, vol. 15, no. 1, pp. 32–44, 2002.
[21] J. Majernik *et al.*, "Normative human gait databases," *Statistics Research Letters*, vol. 2, no. 3, pp. 69–74, 2013.
[22] V. Vapnik, "Statistical learning theory new york," *NY: Wiley*, 1998.
[23] V. Vapnik, *The nature of statistical learning theory*. Springer science & business media, 2013.
[24] B. Schölkopf, "Max planck institute for intelligent systems,"
[25] F. Pedregosa, G. Varoquaux, A. Gramfort, V. Michel, B. Thirion, O. Grisel, M. Blondel, P. Prettenhofer, R. Weiss, V. Dubourg, *et al.*, "Scikit-learn: Machine learning in python," *Journal of machine learning research*, vol. 12, no. Oct, pp. 2825–2830, 2011.
[26] A. Tognetti, F. Lorussi, N. Carbonaro, and D. De Rossi, "Wearable goniometer and accelerometer sensory fusion for knee joint angle measurement in daily life," *Sensors*, vol. 15, no. 11, pp. 28435–28455, 2015.
[27] P. T. Gibbs and H. Asada, "Wearable conductive fiber sensors for multi-axis human joint angle measurements," *Journal of neuroengineering and rehabilitation*, vol. 2, no. 1, p. 7, 2005.
[28] C. Mattmann, F. Clemens, and G. Tröster, "Sensor for measuring strain in textile," *Sensors*, vol. 8, no. 6, pp. 3719–3732, 2008.
[29] "Smartex." http://www.smartex.it/en/. Accessed: 2018-12-17.
[30] "biosignalsplux — wearable body sensing platform." https://www.biosignalsplux.com/en/ang-goniometer. Accessed: 2018-12-17.
[31] "Stretchsense - stretch sensors." https://www.stretchsense.com/stretch-sensors/. Accessed: 2018-12-17.
[32] T. Seel, J. Raisch, and T. Schauer, "Imu-based joint angle measurement for gait analysis," *Sensors*, vol. 14, no. 4, pp. 6891–6909, 2014.